High-Speed, High-Responsivity, and High-Power Performance of Near-Ballistic Uni-Traveling-Carrier Photodiode at 1.55-μm Wavelength

J.-W. Shi, Y.-S. Wu, C.-Y. Wu, P.-H. Chiu, and C.-C. Hong

***Abstract*—In this letter, we demonstrate a novel photodiode at a 1.55-μm wavelength: the near-ballistic uni-traveling-carrier photodiode (UTC-PD). After a p^+ delta-doped layer was inserted into the collector of a UTC-PD, near-ballistic transport of photogenerated electrons under high reverse bias voltage (-5 V) and a high output photocurrent ($\sim$30 mA) was observed. The demonstrated device has been combined with an evanescently coupled optical waveguide to attain high responsivity and high saturation power performance. Extremely high responsivity (1.14 A/W), a high electrical bandwidth (around 40 GHz), and a high saturation current-bandwidth product (over 1280 mA $\cdot$ GHz, at 40 GHz) with high saturation radio-frequency power (over 12 dBm at 40 GHz) have been achieved simultaneously at a 1.55-μm wavelength.**

***Index Terms*—Evanescent coupling, high efficiency, high-power photodiode, optical receivers, photodiode.**

THE performance of microwave and millimeter-wave photonic systems would benefit from the use of photodiodes (PDs) with high saturation power, high-speed performance, and high responsivity [1], [2]. In order to meet these three requirements simultaneously, several technologies have been demonstrated, such as evanescently coupled waveguide PDs [3], [4], partially depleted absorber PDs [5], [6], and uni-traveling-carrier PDs (UTC-PDs) [1], [2]. The structure of UTC-PD has attracted much attention due to its excellent speed and output power performance [1]. However, such a device usually suffers from the problem of bandwidth degradation under high dc external bias voltage [7] due to both the high electric field existing at the junction of the collector (C) and photoabsorption (P) layer, and the decrease in the overshoot drift-velocity of photogenerated electrons [7]. One possible way to enhance the speed performance of UTC-PD is to reduce the externally applied bias voltage and let the value of the electric field in the C-P junction approximately for the critical field, which will enhance the drift-velocity of photogenerated electrons [7]. However, under such low reverse bias voltage (around -1 V for 200-nm collector), the field-screening effect, which originates from the difference in polarity between the output ac voltage across the standard 50-Ω load and the dc bias voltage, will seriously limit the maximum output photocurrent of the UTC-PD [7]. In this work, we demonstrate the state-of-the-art performance of a novel photodiode: the near-ballistic UTC-PD (NBUTC-PD). By inserting an additional p^+ delta-doped layer in the collector of a traditional UTC-PD, we can achieve near-ballistic transport under high reverse bias voltage (-5 V) and a high output photocurrent ($\sim$30 mA). The demonstrated novel device has been combined with the evanescently coupled waveguide structure [3], [4] to attain very high responsivity performance.

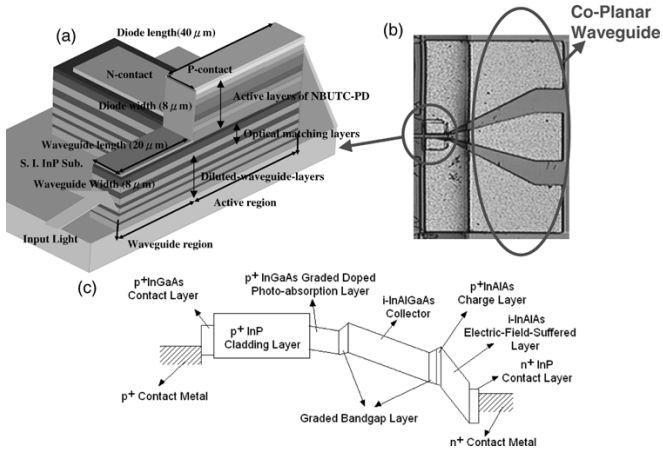

Fig. 1. (a) Cross-sectional view, (b) top view, and (c) conceptual band diagram of the demonstrated NBUTC-PD, which incorporates with an evanescently coupled optical waveguide.

Fig. 1(a) and (b) shows cross-sectional and top views of the demonstrated NBTUC-PD, respectively. Fig. 1(c) shows a conceptual band diagram of the active layers of the whole device. As shown in Fig. 1(c), the thickness of the p-type graded doped $In_{0.53}Ga_{0.47}As$ photoabsorption layer is 150 nm. We adopted an $In_{0.52}Al_{0.15}Ga_{0.33}As$ layer with a 140-nm thickness as the collector layer to enhance the optical coupling process between the diluted-waveguide layers and photoabsorption layer, as shown in Fig. 1(a). The thicknesses of the $In_{0.52}Al_{0.48}As$-based electric field suffer layer (E) and undoped graded bandgap layer at the P-C and C-E junction are 100, 20, and 40 nm, respectively. The total effective collector layer thickness can, thus, be considered to be 300 nm. By introducing a depleted p^+ delta-doped charge layer with a 1×10^{18} cm^{-3} doping density and 5-nm thickness, we can control the maximum electric field in the $In_{0.52}Al_{0.15}Ga_{0.33}As$ collector layer so as to produce an appropriate value (around 40 kV/cm at -5-V bias) needed to sustain an overshoot velocity of photogenerated electrons under certain ranges of the bias voltage and output photocurrent. A very similar epi-layer-design concept has been successfully

Manuscript received March 4, 2005; revised May 9, 2005. This work was supported by the National Science Council of Taiwan under Grant NSC-95-2215-E-008-003 and by the Department of Industrial Technology, the Ministry of Economic Affairs, under Grant 93-EC-17-A-07-S1-0001.

J.-W. Shi, Y.-S. Wu, C.-Y. Wu, and P.-H. Chiu are with the Department of Electrical Engineering, National Central University, Taoyuan 320, Taiwan, R.O.C. (e-mail: jwshi@ee.ncu.edu.tw).

C.-C. Hong is with the Chughwa Telecom. Co., Ltd. Telecom. Laboratory, Taoyuan 320, Taiwan, R.O.C.

Digital Object Identifier 10.1109/LPT.2005.853296

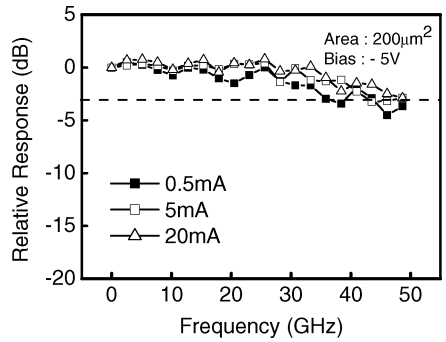

Fig. 2. Measured frequency responses of the device with a 200-μm^2 active area under different levels of the output photocurrent and a fixed dc bias voltage (-5 V). (Square: 0.5 mA; open square: 5 mA; open triangular: 20 mA.)

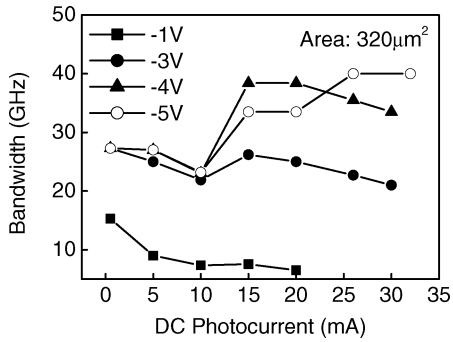

Fig. 3. Electrical bandwidth versus photocurrent under different bias voltages of the device with a 320-μm^2 active area. (Square: -1 V; circle: -3 V; triangle: -4 V; open circle: -5 V.)

implemented in the collector of an AlGaAs–GaAs-based heterojunction bipolar transistor [8]. The optical waveguide structure of our demonstrated NBUTC-PD is based on the reported high-performance planar evanescently coupled photodiode [3]. The employed optical refractive indexes and optical absorption constants of InAlGaAs or InGaAsP quaternaries in our beam-propagation-method (BPM) optical waveguide simulation can be found in [9] and [10]. As shown in Fig. 1(a), we adopted a short (20 μm) multimode waveguide that consists of a diluted waveguide and two optical matching layers [3]. The diluted waveguide is composed of seven $In_{0.86}Ga_{0.14}As_{0.3}P_{0.7}$ layers with 50-, 80-, 110-, 140-, 170-, 200-, and 580-nm thicknesses, interspersed between the 150-nm-thick InP layers. The two optical matching layers are n^+-doped $In_{0.52}Al_{0.48}As$ and $In_{0.52}Al_{0.17}Ga_{0.31}As$ (1×10^{18} cm^{-3}) with 0.6- and 0.3-μm thicknesses, respectively. Although the thick (0.6 μm) $In_{0.52}Al_{0.48}As$ layer has a lower refractive index than the bottom $In_{0.86}Ga_{0.14}As_{0.3}P_{0.7}$ layer, according to our simulation results, this distribution of refractive indexes in our structure greatly enhances the optical absorption process. The epitaxial layers of the demonstrated devices were grown by means of metal–organic chemical vapor deposition on a semi-insulating InP substrate. The detail fabrication process and geometric structure of this device are similar to those of our previous evanescently coupled photodiodes, described in [11].

We employed a tunable semiconductor laser as the light source for dc photocurrent measurement. The center wavelength of this laser was fixed at 1550 nm during dc measurement. Extremely high responsivity of 1.01 and 1.02 A/W was achieved with 150- and 200-μm^2 active areas, respectively. The responsivity of the device with an 8-μm waveguide/diode width and 40-μm (320-μm^2 active area) absorption length could be further improved to 1.14 A/W. The TE/TM polarization dependence of the measured responsivity was around 0.8 dB with a 40-μm absorption length. To our knowledge, these are the highest values ever reported for the responsivity of high-speed and high-power UTC-PDs [1], [2]. The bandwidth and saturation current were measured with a heterodyne beating system [11]. Fig. 2 shows the typical frequency responses of the device with a 200-μm^2 active area under different levels of the output photocurrent (0.5, 5, and 20 mA) and a fixed dc bias voltage (-5 V). One can clearly see that under 0.5- and 5-mA operation, the electrical bandwidth was around 40 GHz. When the photocurrent reached 20 mA, the bandwidth of device increased to 50 GHz. In order to clearly characterize the dynamic behaviors of the NBUTC-PD while avoiding any serious influence of the system-limited bandwidth ($\sim$50 GHz), we measured and analyzed the speed performance of the device with a 320-μm^2 active area and a smaller $f_{3\,\mathrm{dB}}$ bandwidth than that of a 200-μm^2 device under different operation conditions. Fig. 3 shows the measured $f_{3\,\mathrm{dB}}$ electrical bandwidth versus the output photocurrent under different reverse bias voltages. As the diagram indicates, the bandwidth increased significantly when the reverse bias was over -1 V due to the depletion of the charge layer and the reduction of the electron transport time in the collector layer. In each trace, there is an optimum value of the photocurrent for achieving maximum bandwidth performance. When the dc bias voltage was -5 V, the value of the optimum photocurrent reached 30 mA with a 40-GHz electrical bandwidth. The observed bias dependent phenomenon can be possibly attributed to the velocity overshoot of electrons in the collector layer [7], [12] instead of the reported diffusion-velocity enhancement in the p-type photoabsorption layer of the UTC-PD [1], [13], which has a much thicker photoabsorption layer (450 versus 150 nm), and larger variation in the diffusion time of electrons than that of our device [12], [13]. According to our simulation results, when the reverse bias voltage is over -2 V, the electric field in the collector is larger than the critical field (10 kV/cm), and the increase of the output photocurrent will result in a reduction of net electric field and enhancement of the drift velocity of electrons. Under a -5-V bias, the photocurrent has to be large to eliminate the excess electric field and achieve near-ballistic transport. The obtained high responsivity (1.14 A/W) and high electrical bandwidth (around 40 GHz) under high output photocurrent operation of the demonstrated device ensures its applicability in a 40-Gb/s fiber communication system. Fig. 4 shows the measured and fitted frequency responses of the device with a 320-μm^2 active area under 10- and 15-mA output photocurrent values. The dc bias voltage was fixed at -4 V. According to our simulation results, the bandwidth improvement under high current operation (15 mA) is associated to the reduction of the transport time as discussed above and the ac capacitance [12]. The total capacitance is reduced due to the subtraction of the differential ac capacitance $I_C \times (d\tau_C/dV_{\mathrm{ac}})$, proportional to the current, from the depletion capacitance [12]. Where, V_{ac} is the output ac voltage of device, I_C is the photocurrent, and τ_C is the electron drift time. For the case of demonstrated device, such effect should be significant due to that under near-ballistic transport, the variation of drift velocity (time) versus the electric field

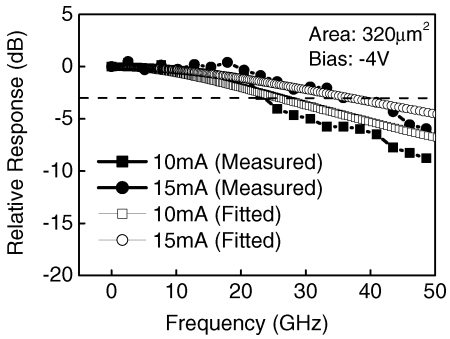

Fig. 4. Measured and fitted frequency responses of the device with a 320-μm^2 active area under different output photocurrent values and a fixed dc bias voltage (-4 V). (Square: measured trace under 10-mA operation; circle: measured trace under 15-mA operation; open square: fitted trace under 10-mA operation; open circle: fitted trace under 15-mA operation.)

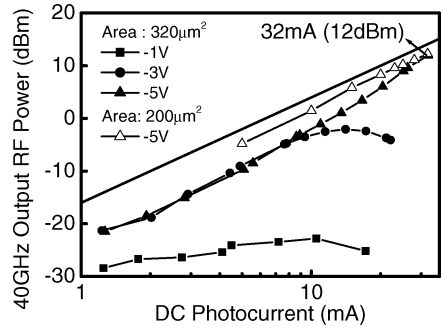

Fig. 5. RF power versus dc photocurrent of the devices with different active areas under different reverse bias voltages (square: -1 V; circle: -3 V; triangle (open triangle): -5 V) at a 40-GHz operating frequency. The ideal relation between the RF power and current on a 50-Ω load is plotted as a straight line for reference purpose.

($V_{\rm ac}$) is obvious, according to the reported field dependence electron drift velocity of III–V semiconductors [9]. The traces shown in Fig. 5 represent the photogenerated radio-frequency (RF) power versus dc photocurrent of the NBUTC-PD under different bias voltages (-1, -3, and -5 V). The operating frequency was fixed at 40 GHz. The ideal relation between the RF power of a 100% modulated large-signal and the average current on a 50-Ω load is also plotted as a straight line for reference. For the case of a -5-V bias, the traces of the device with different active areas (200 and 320 μm^2) are also shown for the purpose of comparison. Since, the bandwidth of the device with a 320-μm^2 active area increases as the photocurrent increases significantly under a -5-V bias, the output RF power is closer to the ideal line than is the case with a low photocurrent. On the other hand, the trace of device with a 200-μm^2 active area under a -5-V bias voltage is very close to the ideal line (less than 3 dB) under both low and high photocurrent operation because the $f_{3\ \rm dB}$ bandwidth of the device is around 40–50 GHz, as shown in Fig. 2. The demonstrated maximum values of the generated RF power and dc photocurrent of the device were limited by the maximum available optical power of our measurement system or the device failure under high current operation (over 30 mA). The obtained values of the maximum RF power (12 dBm) and current (32 mA) of the device with a 320-μm^2 active area were much higher than those reported in previous works on p-i-n evanescently coupled photodiodes with integrated tapers [3], [4]. Furthermore, compared with the state-of-the-art performance achieved with the reported UTC-PD [12], which incorporates with an evanescently coupled waveguide, our demonstrated device can attain higher responsivity (1.14 versus 0.76 A/W) and higher saturation current-bandwidth product (1280 versus 1100 mA $\cdot$ GHz). To our knowledge, this is the highest saturation current and RF power (over 32 mA versus 12 dBm) of a long wavelength photodiode obtained with such high responsivity (1.14 A/W) and such a high electrical bandwidth (40 GHz) [1]–[3].

In conclusion, we have demonstrated a novel photodiode at a 1.55-μm wavelength. Near-ballistic transport of photogenerated electrons has been observed in this device under a high dc bias voltage (-5 V) and high output photocurrent ($\sim$30 mA). State-of-the-art performance has been achieved by using this device with a 320-μm^2 active area, resulting in very high responsivity (1.14 A/W), broad bandwidth ($\sim$40 GHz), and a saturation current of over 32 mA.

REFERENCES

[1] H. Ito, S. Kodama, Y. Muramoto, T. Furuta, T. Nagatsuma, and T. Ishibashi, "High-speed and high-output InP-InGaAs unitraveling-carrier photodiodes," *IEEE J. Sel. Topics Quantum Electron.*, vol. 10, no. 4, pp. 709–727, Jul./Aug. 2004.

[2] K. Kato, "Ultrawide-Band/high-frequency photodetectors," *IEEE Trans. Microw. Theory Tech.*, vol. 47, no. 7, pp. 1265–1281, Jul. 1999.

[3] S. Demiguel, N. Li, X. Li, X. Zheng, J. Kim, J. C. Campbell, H. Lu, and A. Anselm, "Very high-responsivity evanescently coupled photodiodes integrating a short planar multimode waveguide for high-speed applications," *IEEE Photon. Technol. Lett.*, vol. 15, no. 12, pp. 1761–1763, Dec. 2003.

[4] F. Xia, J. K. Thomson, M. R. Gokhale, P. V. Studenkov, J. Wei, W. Lin, and S. R. Forrest, "A asymmetric twin-waveguide high-bandwidth photodiode using a lateral taper coupler," *IEEE Photon. Technol. Lett.*, vol. 13, no. 8, pp. 845–847, Aug. 2001.

[5] X. Li, N. Li, S. Demiguel, X. Zheng, J. C. Campbell, H. H. Tan, and C. Jagadish, "A partially depleted absorber photodiode with graded doping injection regions," *IEEE Photon. Technol. Lett.*, vol. 16, no. 10, pp. 2326–2328, Oct. 2004.

[6] Y. Muramoto and T. Ishibashi, "InP/InGaAs pin photodiode structure maximizing bandwidth and efficiency," *Electron. Lett.*, vol. 39, no. 24, 27, pp. 1749–1750, Nov. 2003.

[7] N. Shimizu, N. Watanabe, T. Furuta, and T. Ishibashi, "InP-InGaAs unitraveling-carrier photodiode with improved 3-dB bandwidth of over 150 GHz," *IEEE Photon. Technol. Lett.*, vol. 10, no. 3, pp. 412–414, Mar. 1998.

[8] T. Ishibashi and Y. Yamauchi, "A possible near-ballistic collection in an AlGaAs/GaAs HBT with a modified collector structure," *IEEE Trans. Electron Devices*, vol. 35, no. 4, pp. 401–404, Apr. 1988.

[9] M. Levinshtein, S. Rumyantsev, and M. Shur, *Handbook Series on Semiconductor Parameters*, Singapore: World Scientific, 1996.

[10] J.-W Pan, J.-L Shieh, J.-H Gau, and J.-I Chyi, "The study of the optical properties of $In_{0.52}(Al_xGa_{1-x})_{0.48}As$ by variable angle spectroscopic ellipsometry," in *Proc. Indium Phosphide and Related Materials (IPRM) Conf.*, May 1995, pp. 245–248.

[11] Y.-S. Wu, J.-W. Shi, J.-Y. Wu, F.-H. Huang, Y.-J. Chan, Y.-L. Huang, and R. Xuan, "High performance evanescently edge coupled photodiodes with partially p-doped photo-absorption layer at 1.55 μm wavelength," *IEEE Photon. Technol. Lett.*, vol. 17, no. 4, pp. 878–880, Apr. 2005.

[12] M. Achouche, V. Magnin, J. Harari, F. Lelarge, E. Derouin, C. Jany, D. Carpentier, F. Blache, and D. Decoster, "High performance evanescent edge coupled waveguide unitraveling-carrier photodiodes for $>$ 40-Gb/s optical receivers," *IEEE Photon. Technol. Lett.*, vol. 16, no. 2, pp. 584–586, Feb. 2004.

[13] N. Li, X. Li, S. Demiguel, X. Zheng, J. C. Campbell, D. A. Tulchinsky, K. J. Williams, T. D. Isshiki, G. S. Kinsey, and R. Sudharsansan, "High-saturation-current charge-compensated InGaAs-InP uni-traveling-carrier photodiode," *IEEE Photon. Technol. Lett.*, vol. 16, no. 3, pp. 864–866, Mar. 2004.